Biosensors and Bioelectronics 198 (2022) 113804

Contents lists available at ScienceDirect

Biosensors and Bioelectronics

journal homepage: www.elsevier.com/locate/bios

Continual and accurate home monitoring of uric acid in urine samples with uricase-packaged nanoflowers assisted portable electrochemical uricometer

Xiuguang Xing [a,1], Bangben Yao [b,1], Qian Wu [a], Ru Zhang [a], Li Yao [a], Jianguo Xu [a], Guangheng Gao [c], Wei Chen [a,*]

[a] Engineering Research Center of Bio-process, MOE, School of Food and Biological Engineering, Intelligent Manufacturing Institute, Hefei University of Technology, Hefei, 230009, China
[b] Anhui Province Institute of Product Quality Supervision & Inspection, Hefei, 230051, PR China
[c] Key Laboratory for Biosensors of Shandong Province, Shandong Academy of Sciences, Jinan 250353, China

ARTICLE INFO

Keywords:
Uric acid monitoring
Screen printed electrodes
Uricase-inorganic hybrid nanoflowers
Portable biosensor
Home-test

ABSTRACT

A convenient, fast and non-invasive portable electrochemical uricometer (PUM) assisted with the uricase-packaged nanoflowers (NFs) was constructed for continually and accurately monitoring of uric acid (UA) in urine samples at random intervals in just 20 s. Only a small amount of urine (50 μL) was needed for each test. Electrochemical deposition was adopted to modify gold nanoparticles (AuNPs) on screen-printed carbon electrodes (SPCE) and uricase-inorganic hybrid NFs (UOx-NFs) induced by calcium ions (Ca^{2+}) were introduced for UA detection with expected specificity. Cyclic voltammetry (CV) (detection limit of 8.87 μM and liner range of 0–4 mM) and amperometry (detection limit of 0.82 μM and liner range of 0–5 mM) protocols were studied for UA detection, respectively. Finally, the uric acid in urine had be successfully continually monitored from volunteers with various dietary choosing, the results of which can be adopted as the effective evidence for uric acid control.

1. Introduction

Uric acid (UA, $C_5H_4N_4O_3$) is the main metabolite of purine derivatives in human. Under normal conditions, UA in serum ranges from 0.24 to 0.52 mM and from 1.4 to 4.4 mM in urine (Ponnaiah et al., 2018). In addition, most of UA in human body is excreted through the kidney (Dalbeth and Merriman, 2009). Usually, the whole UA excretion value is 250–750 mg/day, which accounts for about 70% of the daily UA excretion. And it has also been proved that 90% of hyperuricemia was related to the decreased renal UA excretion (Dalbeth et al., 2019). The abnormal UA level in human body can further induce the serious gout, kidney disease, and even Lesch-Nyhan syndrome etc (Nishida, 1992).

Urinalysis is the clinical adopted standard method for diagnosing gout, Lesch-Nyhan syndrome, and hyperuricemia. A variety of methods for detection UA in urine have been reported, such as fluorescence analysis (Fang et al., 2016; Xin et al., 2017), colorimetry (Huang et al., 2018; Lu et al., 2017; Miller and Oberholzer, 1990; Wang et al., 2019), chemiluminescence (Saqib et al., 2018; Sheng et al., 2017; Vakh et al., 2017; Yang and Zhang, 2010), high-performance liquid chromatography/mass spectrometry (Perelló et al., 2005), capillary electrophoresis-amperometry (Xu et al., 1997), and ion chromatography (Zhao et al., 2011). However, these methods were all highly depended on the expensive instruments. Previous studies have also demonstrated that the electrochemical protocols have been widely applied for UA analysis due to the sensitivity and speed (Fang et al., 2011; Li et al., 2012; Revin and John, 2011; Wang et al., 2007; Zen and Hsu, 1998). Usually, these electrochemical protocols for UA determination can be categorized as the enzymatic and non-enzymatic methods (Erden and Kilic, 2013). The non-enzymatic method is convenient, fast and low-cost. However, the biggest obstacle of non-enzymatic method is the detection can be easily interfered by the presence of ascorbic acid, dopamine, NADH and other common biological molecules in the complicated body fluids (Sun et al., 2016). Recently, some nanomaterial-modified protocols have achieved great progress in anti-interference ability (Wang et al., 2018; Gao et al., 2018). However, these methods still need complicated modification and detection procedures. Comparatively, the enzymatic protocols have the overwhelming advantages in both the specificity and anti-interference

* Corresponding author.
E-mail address: chenweishnu@163.com (W. Chen).
[1] These two authors contributed equally to this work.

https://doi.org/10.1016/j.bios.2021.113804
Received 22 August 2021; Received in revised form 20 October 2021; Accepted 13 November 2021
Available online 17 November 2021

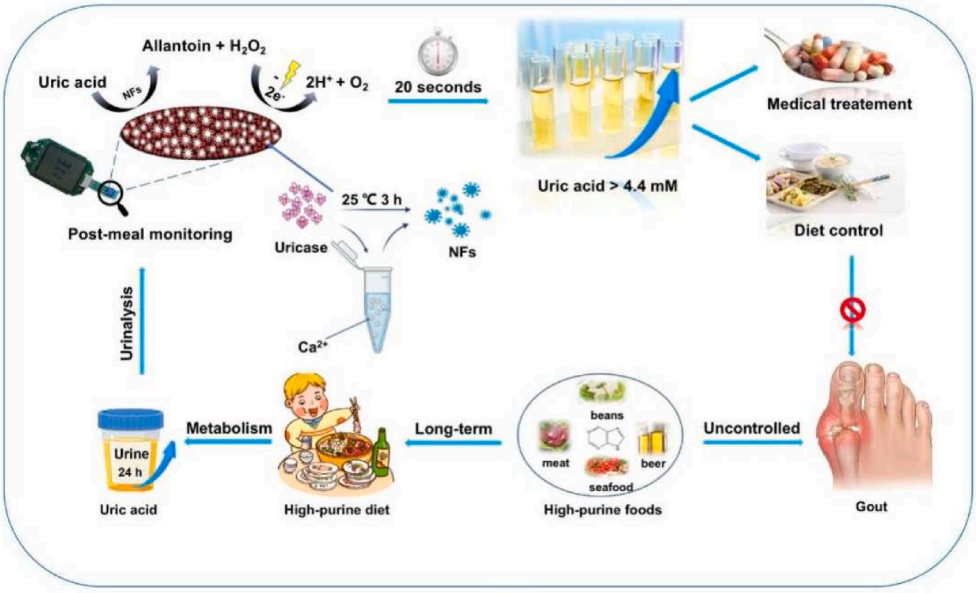

Scheme 1. The UOx decorated nanoflowers based uricometer for home monitoring of UA in urine samples and diet management.

ability due to the excellent properties of uricase (UOx) (Grieshaber et al., 2008; Verma et al., 2019; Shi et al., 2020). Similarly, complicated materials preparation processes and electrode modifications were required, and all electrodes can only be one-time using. Of great note, all these methods cannot be performed for the routine home monitoring for the noninvasive samples.

Recently, the portable electrochemical biosensor has been constructed and commercialized for UA detection in blood (Lou et al., 2018b; Paraskos et al., 2015). However, repeated invasive finger punctures for blood test will cause the inconvenience and the pain to the tested subjects inevitably, which hamper the daily monitoring of UA at home to certain extent. Fortunately, the UA in urine is also adopted as the effective index for evaluation of UA excretion in 24 h. Therefore, non-invasive continual detection of UA in urine can provide a direct and valuable reference for effective control of high-purine diets and the 24-h detection of UA in urine can be used to distinguish the decreased or increased UA excretion of the tested subjects, which is extremely critical for the accurate clinical diagnosis of hyperuricemia and gout.

Therefore, the UOx-NFs which has better stability than free-UOx (Ge et al., 2012; Ye et al., 2016; Zeinhom et al., 2018; Hao et al., 2019; Huang et al., 2018; Fukuda et al., 2020; Miland et al., 1996) assisted portable electrochemical uricometer (PUM) was constructed for direct and continual detection of UA in non-invasive urine samples with good stability, high sensitivity in less than 20 s. The clinical urine samples of different volunteers have also been well monitored and analyzed with the constructed PUM. All the UOx-NFs preparation and sensing electrode modifications can be easily produced in batch, which holds the great potential in practical home UA monitoring.

2. Experimental

2.1. Materials and chemicals

Phosphate buffer saline (20xPBS, pH 7.4, Cell Culture Grade), UA assay kit (Colorimetry, Sangon, Shanhgai), UOx (produced by Candida utilis, 4.41U/mg) was purchased from Shanghai Bioengineering Co., Ltd. Anhydrous calcium chloride, potassium ferricyanide and potassium ferrocyanide, potassium chloride, UA were purchased from Aladdin Reagent Company (Shanghai, China). D-ascorbic acid, dopamine, sucrose, glucose, L-fructose, L-cysteine, and L-lysine were purchased from Sinopharm Chemical Reagent Company (Shanghai, China). Nafion-117 solution (~5% in a mixture of lower aliphatic alcohols and water) was purchased from Sigma-Aldrich LLC. Artificial urine: urea 25 g, NaCl 9 g, NH_4Cl 3 g, Creatinine 2 g, Na_2HPO_4 2.5 g, KH_2PO_4 2.5 g, Na_2SO_4 2.25 g, all reagents were dissolved in 1 L ultrapure water and adjusted pH to 7.2 using NaOH solution. The resistivity of ultrapure water (Milli-A10 system, Millipore) was 18.2 Ω/cm and used throughout the experiment.

2.2. Instruments

The CHI650D electrochemical workstation was purchased from Shanghai CH Instrument Co., Ltd. (Shanghai. China) The SPCE with a three electrodes system (the back plate was 40 mm long, 10 mm wide, and the diameter of circular working electrode was 4 mm). The counter electrode (CE) and work electrode (WE) were graphite carbon electrode while the reference electrode (RE) was Ag/AgCl. The handheld low-power electrochemical sensor platform was customized according to our requirements. The parameters of the handheld low-power electrochemical platform include the constant voltage of +0.5 V and the current ranges from 0 to 99 μA.

2.3. Preparation of AuNPs decorated sensing surface

Electrodeposition is a cheap, fast, and simple technique for controlled deposition of nanoparticles (Zhao et al., 2020). Typically, in this research, to achieve the best stability of SPCE, SPCEs were firstly sonicated in anhydrous ethanol solution for 30 s. Then, SPCEs were rinsed 3 times with ultrapure water to remove organic impurities on the surface of electrode. 50 μL $HAuCl_4$ (3 mM) was dropped onto the electrode surface and the AuNPs were deposited at a constant voltage of −0.4 V vs Ag/AgCl for 50 s. Afterward, the AuNPs-SPCE was rinsed with ultrapure water to remove excess $HAuCl_4$ and electrochemical cleaned (CV, −0.2-0.6 V, 50 mV/s, 20 cycles) in 5 mM Zobell so that the unbound AuNPs and other impurities on the surface of SPCE can be removed. Finally, the AuNPs decorated SPCE (AuNP-SPCE) was rinsed three times with ultrapure water for subsequent research.

2.4. Preparation of UOx-NFs and NFs-AuNPs-SPCE

UOx-NFs were prepared according to the reported method with slight modification (Ge et al., 2012). Typically, 20 μL $CaCl_2$ (0.2 M) solution was added to 1 mL 5 mM PBS (pH 7.4) containing 0.25 mg UOx.

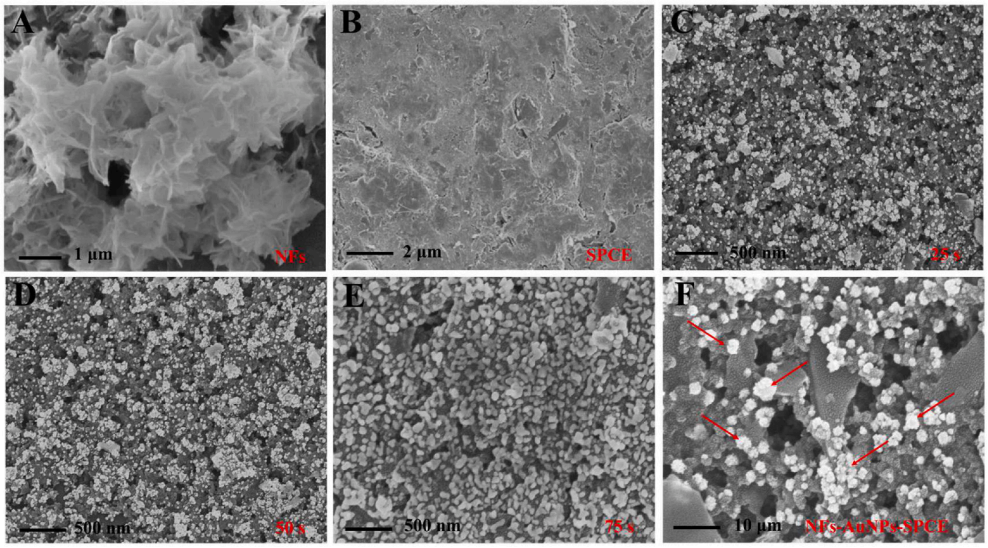

Fig. 1. (A) FE-SEM image of UOx-NFs. (B) FE-SEM image of SPCE. (C–E) FE-SEM images of electrochemical deposition (−0.4 V vs Ag/AgCl) of gold nanoparticles on WE for 25 s, 50 s and 75 s. (F) FE-SEM images of NFs-AuNPs-SPCE. (For interpretation of the references to color in this figure legend, the reader is referred to the Web version of this article.)

The mixture was incubated at room temperature for 3 h and the supernatant was removed by centrifugal at 8000 rpm for 5 min. The NFs precipitates were washed with ultrapure water for 3 times and finally resuspend in 200 μL ultrapure water and stored at 4 °C.

In order to decrease the complexity of the construction of portable uricometer, direct dripping coating strategy was used to preparation of NFs-AuNPs-SPCE (Khue et al., 2020). In detail, the above prepared UOx-NFs were mixed thoroughly with the shaker and then 8 μL UOx-NFs was dropped onto the AuNP-SPCE (WE). The NFs-AuNPs-SPCE was dried at room temperature and stored at 4 °C for subsequent measurement research. Each modification step was characterized by CV (scan rate of 50 mV/s, −0.2 V–0.6 V) and EIS (scan amplitude of 10 mV, 0.01 Hz-50 kHz) in 5 mM Zobell to confirm the functionalization of the WE. In order to compare the stability of UOx-AuNPs-SPCE and NFs-AuNPs-SPCE, we prepared UOx-AuNPs-SPCE using similar dripping coating strategy. First, 8 μL 1 mg/mL UOx was dropped onto AuNPs-SPCE, and then the UOx was immobilized using 0.5% Nafion solution.

2.5. Electrochemical measurement studies

The UA detections were performed with both CHI 650D workstation and self-constructed PUM, respectively. For the electrochemical detections with the CHI 650D workstation, 50 μL UA sample was loaded on the NFs-AuNPs-SPCE. Typically, the CV was performed with a 50 mV/s scan rate in the potential range from −0.2 V to 0.6 V. The amperometric protocol was conducted at a constant potential of +0.5 V vs Ag/AgCl for sweeping 300 s. Following, for UA detection with portable PUM, urine samples were firstly collected in the 4 mL centrifuge tube. Then, the NFs-AuNPs-SPCE was inserted into the collected urine sample immediately after the NFs-AuNPs-SPCE was loaded to the self-constructed PUM. The current value was recorded after 20 s and the exact current value at 20 s was adopted for quantitative analysis. For the continual and real-time monitoring of UA in the volunteers' urine samples, the urine samples will be tested immediately after the volunteers consumed tofu, chicken, beef, and beer and other high-purine foods.

3. Results and discussion

3.1. The sensing mechanism of UA

As depicted in Scheme 1, the UOx was loaded into the NFs to protect its activity. The UA was catalyzed by UOx-NFs immobilized on AuNPs-SPCE to produce the allantion, CO_2 and H_2O_2, H_2O_2 can be measured by CV or amperometry protocol. The detailed UOx-based catalytic reaction equation is as follows:

$$UA + H_2O + O_2 \xrightarrow{Uricase} \text{allantion} + CO_2 + H_2O_2 \quad (1)$$

$$H_2O_2 \xrightarrow{Electrocatalysis} 2H^+ + O_2 + 2e^- \quad (2)$$

3.2. Characterization of UOx-NFs and functionalized WE

The UOx-NFs were firstly characterized by field emission scanning electron microscope (FE-SEM). Results in Fig. 1A shows the distinguishable flower-like shape of the UOx-decorated nanocomposite with average size of 2 μm. Then, the UOx-NFs were modified on the WE directly and easily by drop casting method. The WE was firstly confirmed as shown in Fig. 1B, demonstrating the comparable smooth layered structure of the graphitic carbon. To improve the sensing performance, AuNPs were *in-situ* deposited on the WE before immobilization of UOx-NFs. When a −0.4 V voltage vs Ag/AgCl was applied on the WE, the oxidation state Au^{3+} ions were reduced to gold atoms and deposited on the WE. After a short while, more and more gold atoms were deposited on the WE to form AuNPs. The electrochemical reaction equation of AuNPs deposition is described as:

$$[AuCl_4]^- + 3e^- \rightarrow Au\ (0) + 4Cl^- \quad (3)$$

$$[AuCl_4]^- + 2e^- \rightarrow [AuCl_2]^- + 2Cl^- \quad (4)$$

$$[AuCl_2]^- + e^- \rightarrow Au\ (0) + 2Cl^- \quad (5)$$

The *in-situ* deposition of AuNPs on WE were also observed with FE-SEM. Results in Fig. 1C–E are the typical images of AuNPs deposited for 25 s (24.69 nm, SD = 4.1, n = 20), 50 s (45.23 nm, SD = 3.8, n = 20) and 75 s (100.43 nm, SD = 13.37, n = 20), respectively. It is easy to find that there are still many blank sites on the surface of WE after 25 s deposition (Fig. 1C) while 75 s deposition induces the linkage among the formed AuNPs with the sacrifice of surface area for subsequent UOx-NFs immobilization (Fig. 1E). Meanwhile, the increased deposition time also increases the diameter of the formed AuNPs. Deposition of 50 s can provide numerous separated AuNPs with the diameter of 45 nm for uricase immobilization (Fig. 1D). Finally, the UOx-decorated NFs can be well immobilized on the surface of the WE through the electrostatic

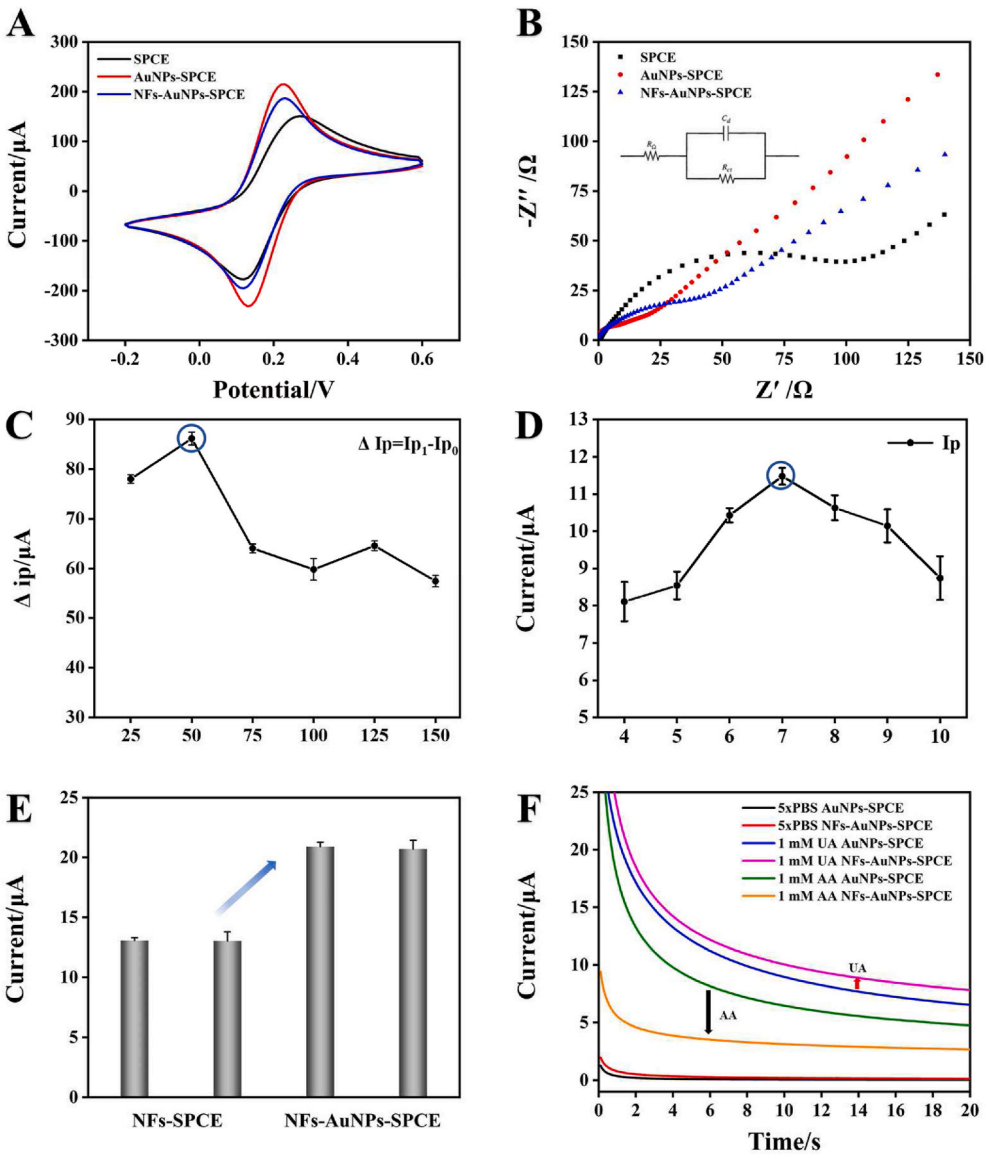

Fig. 2. (A) EIS and (B) CV characterization of SPCE at different modification stages. (C) AuNPs deposition time optimization (−0.4 V vs Ag/AgCl). (Ip_0: peak current before AuNPs deposition. Ip_1: peak current after AuNPs deposition). (D) The effect of buffer pH on NFs-AuNPs-SPCE. (E) Current signal response (+0.5 V vs Ag/AgCl) of NFs-SPCE and NFs-AuNPs-SPCE in 2 mM UA. (F) Amperometric curves (+0.5 V vs Ag/AgCl, 20 s) of AuNPs-SPCE and NFs-AuNPs-SPCE in 1 mM UA and 1 mM AA.

adsorption of gold and the physical entrapment of the gaps, maintaining the good shape as demonstrated in Fig. 1F. The electrochemical characterizations of the AuNPs deposition were also carried out step by step and detailed results were shown in Fig. S1. Meanwhile, energy dispersive X-ray detector (EDX) has also been adopted for the characterization of AuNPs deposition on SPCE. Results in Fig. S2 well demonstrated the presence of gold elements on the surface of electrode, indicating the successful deposition of AuNPs on the SPCE. All results can well demonstrate the successful deposition, good immobilization stability of the AuNPs and NFs, and improved sensing performance after AuNPs deposition on the surface of the WE. And all related functionalization procedures including the NFs preparation, gold deposition and electrode modification can be conducted in the scale-up mode, which will benefit the final practical applications in non-invasive UA detection for personal health monitoring.

Furthermore, CV and Electrochemical Impedance Spectroscopy (EIS) were also performed to confirm the deposition of AuNPs and immobilization of NFs. It can be seen from Fig. 2A that the SPCE has a peak current (Ip = 150.9 μA) in 5 mM Zobell while 214.7 μA for the AuNPs-SPCE, which can be ascribed to the increased surface area after the deposition of AuNPs on the SPCE. The current was slightly decreased to 186.7 μA after immobilization of NFs, which can be ascribed to the comparable poor conductivity of protein components in uricase-inorganic-hybrid NFs. The impedance behaviors of the biosensor during the modification process were also studied. EIS data was processed by Zview software, the equivalent circuit of the NFs-AuNPs-SPCE was simulated and the Rct values of the electrodes were calculated. As we can see from Fig. 2B, the SPCE displays a large semicircle with a very high electron transfer resistance (Rct, 150.24 Ω). The subsequent deposition of AuNPs results in a significant decrease of Rct (8.74 Ω), implying that AuNPs deposition has better electrical conductivity accelerating the electron transfer in the electrochemical reaction. After immobilization of NFs on the AuNPs-SPCE, the NFs generates a weak conductive layer that blocks the electron transferring, to a certain extent, which is clearly indicated by the slight increase of Rct (62.18 Ω). EIS results also demonstrated the consistent conclusion with CV characterization.

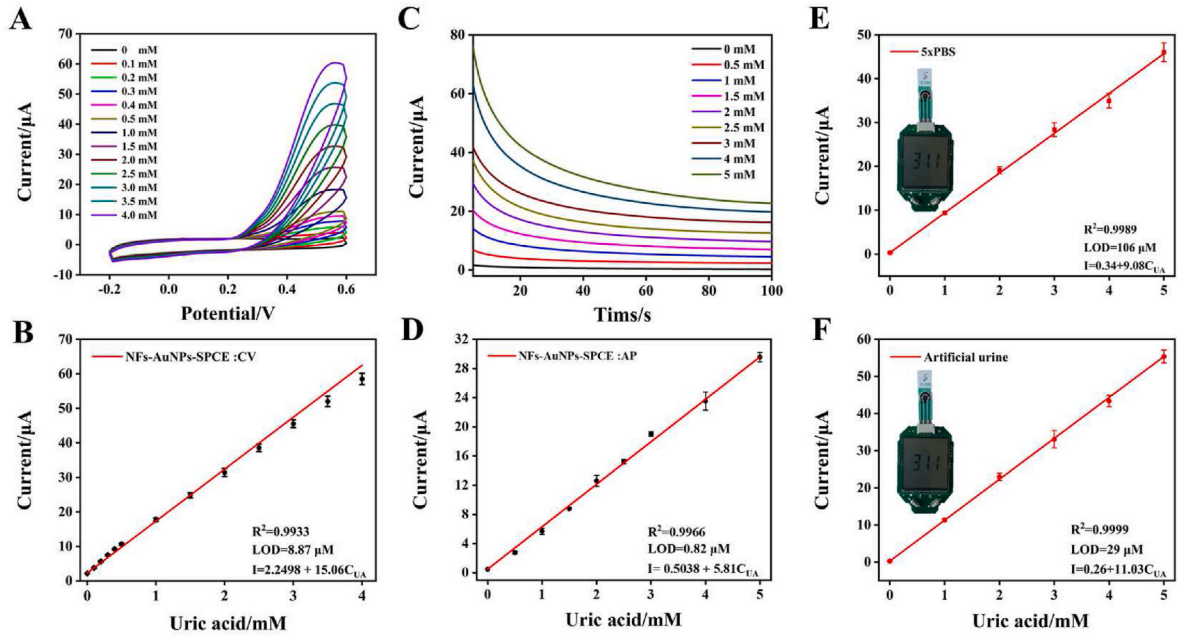

Fig. 3. (A) CV and (C) amperometry measurements of NFs-AuNPs-SPCE 0–4 mM or 0–5 mM of UA in 5xPBS. Plot of the (B) CV (+0.5 V vs Ag/AgCl) and (D) amperometry (+0.5 V vs Ag/AgCl, 20 s) intensity to UA concentration. Current of the PUM intensity to the target UA concentration in 5xPBS (E) and artificial urine (F) with waiting time 20 s after sample loading.

3.3. Optimization of sensing conditions

Based on the NFs-assisted SPCE for UA detection, some important parameters, such as AuNPs deposition time and pH, were carefully considered and optimized. In order to achieve the better conductivity of SPCE, the Ip at different AuNPs deposition time including 25 s, 50 s, 75 s, 100 s, 125 s and 150 s were measured in 5 mM Zobell. Results in Fig. 2C strongly indicate that the maximum peak current (ΔIp = 85 μA) was achieved at 50 s, which is in accordance with the results of SEM and adopted as the optimal time for WE functionalization. After the immobilization of UOx-NFs, the pH of the sensing system was investigated. Results in Fig. 2D demonstrate that pH greatly influenced the sensing performance of the UA biosensor while the best performance was achieved at pH 7.0. And the measured signals are comparable in the range from pH 6.0 to 8.0, which can guarantee the simplicity of practical applications without any treatment of the urine samples.

In order to prove that AuNPs deposition does enhanced the sensing performance of SPCE, the NFs-SPCE and NFs-AuNPs-SPCE were used to detect 2 mM UA solution in 10 mM PBS. It can be seen from Fig. 2E that the sensing current of NFs-AuNPs-SPCE (20.9 μA) increased about 1.55 time compared to NFs-SPCE (13.1 μA), indicating that electron transfer ability of SPCE was enhanced after AuNPs deposition on SPCE. Besides, the UOx-NFs also have important effect on UA sensing performance. Results in Fig. 2F can be analyzed from two aspects: (1) only the target UA can increased current signals compared to the control groups, demonstrating the satisfied specificity of UOx in NFs; (2) among the control groups, taking AA for example, the sensing current was further decreased on the NFs-AuNPs-SPCE compared with the AuNPs-SPCE, indicating the background current signals interference can be effectively eliminated with the modification of UOx-NFs on the AuNPs-SPCE. All these results can well demonstrate the expected properties of functionalized NFs-AuNPs-SPCE for UA detection.

3.4. Investigation of UA sensing performance

Under optimal experimental conditions, the UA detection was firstly carried out by the classic electrochemical station. Results in Fig. 3A–D clearly demonstrate the good sensing performance of both CV and amperometry measurement modes. The linear relationship in the range from 0 to 4 mM with $R^2 = 0.9933$ ($I = 2.25 + 15.06\ C_{UA}$) and 0–5 mM with $R^2 = 0.9966$ ($I = 0.5038 + 5.81\ C_{UA}$) for CV and amperometry, respectively. The limit of detections (LODs) was calculated to be 8.87 μM and 0.82 μM according to the 3σ rule, respectively.

Table 1
Recoveries of UA in human urine based on the PUM.

sample	before (mM)	added (mM)	after (mM)	recovery (%)	RSD (%)
0	*0.82*	*0*	*0.85*	-	*3.45*
1	*0.7*	*0.5*	*1.17*	*98.3*	*3.38*
2	*0.64*	*1*	*1.73*	*107.9*	*5.01*
3	*0.61*	*1.5*	*2.27*	*108.2*	*6.93*

"n = 6″

Based on the parameters for amperometric test with electrochemical station, the PUM with the current sensing range from 0 to 99 μA (corresponding to UA concentration from 0 to 16.95 mM) was constructed and adopted for rapid and direct UA detection using amperometric technology. UA were measured in both 5xPBS and artificial urine samples at different concentrations and the amperometric response was recorded on the PUM. Results in Fig. 3E and F (detailed detection data was given in Tables S1–2) showed that good linear relationship in the range from 0 to 5 mM with $R^2 = 0.9989$ ($I = 0.34 + 9.08C_{UA}$, LOD = 106 μM) and $R^2 = 0.9999$ ($I = 0.26 + 11.03C_{UA}$, LOD = 29 μM) in 5xPBS and artificial urine, respectively, indicating the powerful application potential in routine non-invasive and continual monitoring of UA in urine samples.

The recoveries of UA with PUM were also conducted with the urine samples from the volunteers of our lab. The collected urine samples were firstly measured with the PUM to get the initial concentration of the UA. Then different amount of UA was spiked into the pre-determined samples and the spiked urine samples were measured with PUM again. From results in Table 1, it can be found that the recoveries of UA at low (0.5 mM), medium (1 mM) and high (1.5 mM) concentrations were 98.3%, 107.9% and 108.2%, respectively with the relative standard deviations (RSDs) all less than 7%. These recoveries results in Table 1 clearly indicate the satisfied capabilities for practical application in UA

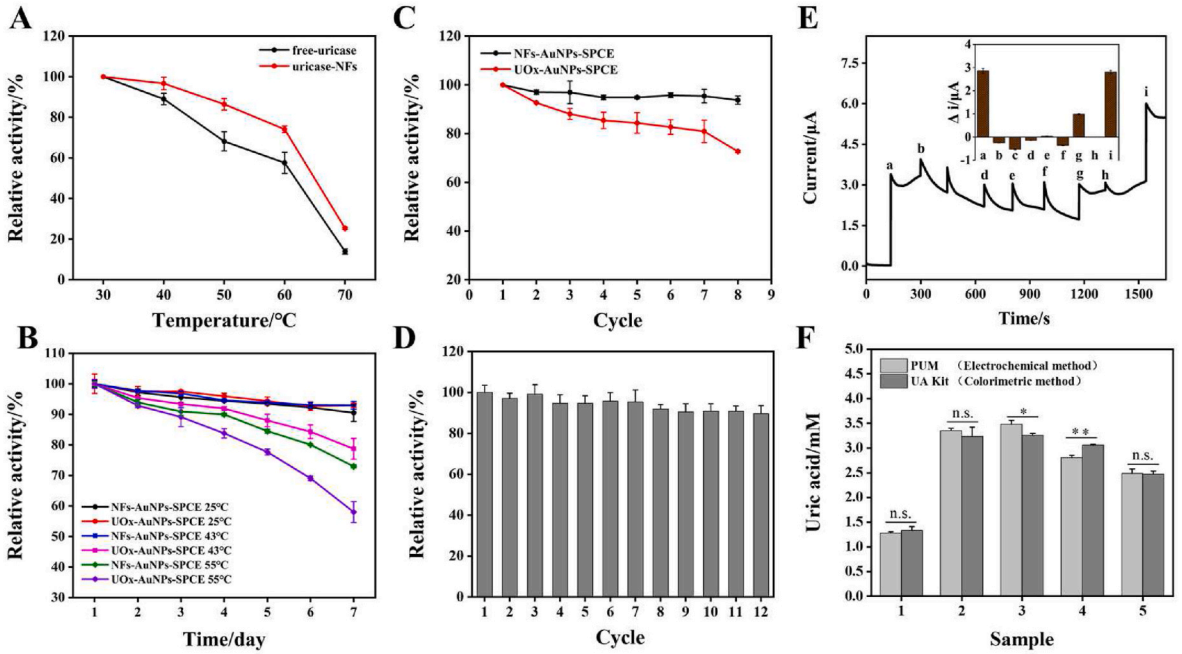

Fig. 4. (A) After 10 min of inactivation at different temperatures, the relationship between the relative enzyme activity and inactivation temperature. (B) The relationship between the storage days at 25 °C, 43 °C or 55 °C and activity retention rate of NFs-AuNPs-SPCE/UOx-AuNPs-SPCE. (C) After UOx-AuNPs-SPCE and NFs-AuNPs-SPCE were repeated used for eight times, the activity retention rate of UOx-AuNPs-SPCE and NFs-AuNPs-SPCE. (D) The change of relative activity after recycling 12 times in an artificial urine sample containing 2 mM UA. (E) Interference experiment of 8 interference substances and 5 μL of each interfering substance was added. (a: UA; b: Sucrose; c: Glucose; d: D-fructose; e: L-cysteine; f: L-lysine; g: L-ascorbic acid; h: Dopamine; i: UA). (F) Comparing between PUM and commercially available UA test kit. (1–4: Actual urine sample; 5: UA standard sample (2.5 mM) provided in the UA test kit). (Asterisks indicate statistical significance using Student's t-test, **P < 0.01 and *P < 0.05, n.s., not significant).

monitoring in urine samples.

3.5. Stability, reusability and anti interference test

The UOx and UOx-NFs were inactivated for 10 min at different temperatures to interrogate the stability of UOx and UOx-NFs. The stability of the UOx-NFs and free-UOx was studied refer to the method reported previously (TMB–H_2O_2–HRP system) (Wang et al., 2020). It can be seen from Fig. 4a that UOx-NFs have better stability than free-UOx. The stability of the UA sensing electrode was further confirmed with the accelerated aging test (Anderson and Scott, 1991; Lou et al., 2018a). In both Fig. 4B and Fig. S2, the sensing performance of the electrode stored at 55 °C for 7 days can maintain the about 75–80% of the fresh prepared electrode. According to the empirical formula of Arrhenius equation and our previous reports with accelerated aging research (Chen et al., 2019, 2020), storage at 55 °C for 14 days corresponds to the storage at 25 °C for one-year. Therefore, all results prove that the shelf-life of the functionalized NFs-AuNPs-SPCE can be at least half a year for UA monitoring with the PUM.

Furthermore, the stability of the immobilized UOx and UOx-NFs on AuNPs-SPCE were compared respectively by repeated measuring of the same urine samples. After each use, the electrode was carefully washed with ultrapure water and dried with washing ear ball for the next measurement. We can see from Fig. 4C that after 8 times repeated measuring, the activity retention rate of UOx-AuNPs-SPCE was gradually decreased and lower than NFs-AuNPs-SPCE while the sensing current of the 8th measurement using NFs-AuNPs-SPCE still maintains more than 95% compared with the 1st measurement. After tested 12 times, almost 90% of the activity was retained for NFs-AuNPs-SPCE as shown in Fig. 4D. This can be due to the protection effect from the multi-dimensional porous structure of NFs and the improved immobilization stability with the deposited AuNPs on the WE. Although the cost of prepared NFs-AuNPs-SPCE is very low (0.1 dollar each) and affordable by the consumers, this excellent reusability will further decrease the cost and widen its application in continual UA home monitoring.

Besides, the specificity or the anti-interference property of the PUM was evaluated. Firstly, 50 μL buffer solution was added to the NFs-AuNPs-SPCE, after the electrode current was stable, 5 μL 2 mM of various interfering substances were added step by step. The stable current before and after adding interfering substances was compared. Results in Fig. 4E show that significant signal response (the i step) can only be induced by UA while other control samples cannot induce any significant signal response (from a to h step). This excellent specificity can be attributed to the adopted UOx assisted catalytic electrochemical sensing mechanism, which also guaranteed the better anti-interference effect for the direct detection of clinical urine samples without any pre-treatments.

3.6. Practical test and continual monitoring of UA in urine samples

The practical UA detection performances were evaluated from two aspects. On one aspect, the collected urine samples were simultaneously measured by both the commercial UA quantification kit and our constructed PUM. As results demonstrated in Fig. 4F, through T-test of five groups data by Origin, it can be found that group 1, 2 and 5 do not have any significant differences (P > 0.05). Although the significant differences in group 3 (P < 0.05) and group 4 (P < 0.01) were observed, the relative standard deviations (RSD) of the these two group as 6.75% and 9.29% respectively were still acceptable for the application. These results well express the high correlation between the commercial kit and the UOx-assisted functional electrode based PUM. In order to verify the reproducibility of the functional electrodes, five different batches of electrodes were used to measure the uric acid solutions at different concentrations. The verification results in Fig. S5 show that these electrodes of different batches have the consistent detection results, indicating the satisfied reproducibility of the fabricated electrodes for practical applications.

On the other aspect, three volunteers' urine samples were analyzed

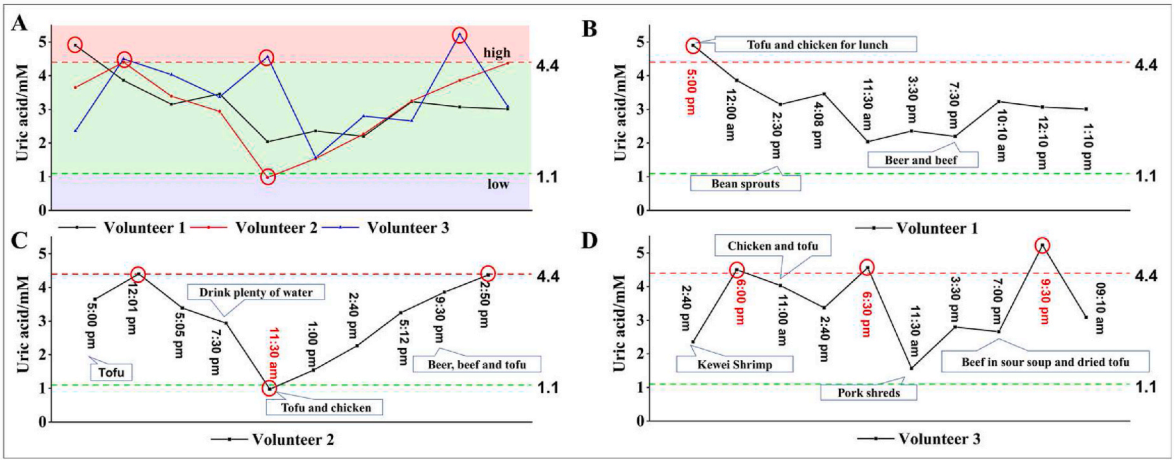

Fig. 5. (A) Three days UA concentration trend chart of urine sample volunteers. (B) The relationship between the UA concentration and the number of urinations after the urine sample volunteer 1 consumed a large amount of soy products. (C) The urine sample volunteer 2 started eating chicken, beef and other high-purine foods and beer without drinking water after a day of low-purine diet. (D) Urine sample volunteer 3 without any diet plan.

with PUM. To ensure accurate measurement results, each electrode was treated as disposable to simulate the practical routine monitoring. Other electrodes of the same batch were stored and sealed in a ziplock bag for using. Each volunteer was continually monitored for more than 72 h. Of note, the UA in the volunteers' urine samples after consumption of high purine or protein foods will be definitely increased and monitored by PUM (Fig. 5). As a control experiment, three volunteers' urine samples were also tested under the condition of normal daily diets without excess amount of high purine foods. As we can see from Fig. S6, the volunteers can maintain the steady-state UA level in urine with the common diets. And the dangerous concentration of UA (higher than the recommended upper limit, 4.4 mM) in urine can be easily monitored and warned with PUM after the high-purine diet or other hyperuricemia related reasons, which will provide the direct and effective evidence for the diet control and disease monitoring. These validation results of practical monitoring of UA in urine samples strongly demonstrated that UOx-NFs assisted PUM has great application potential in routine non-invasive point of care test and home health monitoring. For comparison, we also collected some previous reported UA detection methods based on UOx in recent years and summarized in Table S3. All the detailed comparison results in Table S3 well demonstrate that the reported UOx-NFs-assisted PUM have the obvious superiorities including the sample requirements, the detection limit and hardware for quantitative analysis.

4. Conclusions

Inspired by the most classic and commercialized portable glucose meter (PGM) for blood glucose control, we constructed the uricase-assisted PUM which can provide the valuable proof or advice for the daily diet and disease management. The optimized NFs-AuNPs-SPCE was applied onto the self-made PUM which has great application potential, such as wide linear range (0–5 mM), high sensitivity (LOD = 0.82 μM), excellent anti-interference ability, repeat performance and non-invasive analysis.

The professional test app for continual data collection and calculation of the 24-h UA excretion in body will be developed and related work is ongoing in our lab for the further practical application of this constructed PUM. All research in this study provided a potential and powerful protocol for the non-invasive routine and continual monitoring of UA in urine at home, which will greatly alleviate the burden of blood UA in hospital.

Supporting information

Electrochemical behaviors of SPCE/SPCE-AuNPs/SPCE-AuNPs-NFs, linear curves of UA concentration and absorbance were plotted using colorimetry method, the data of PUM tests in 5xPBS and artificial urine and other information were provided in the supporting information.

Notes

The authors declare that they have no known competing financial interests or personal relationships that could have appeared to influence the work reported in this paper.

CRediT authorship contribution statement

Xiuguang Xing: Investigation, results and writing original draft, Writing – original draft. **Bangben Yao:** Writing original draft, Methodology, Writing – original draft. **Qian Wu:** Methodology, and discussion. **Ru Zhang:** Investigation, and, Validation. **Li Yao:** Methodology, and discussion. **Jianguo Xu:** Reproducibility study. **Guangheng Gao:** hardware preparation. **Wei Chen:** Supervision, Writing- Reviewing and Editing, Writing – review & editing.

Declaration of competing interest

The authors declare that they have no known competing financial interests or personal relationships that could have appeared to influence the work reported in this paper.

Acknowledgements

This study was supported by the grants of Anhui Key R&D Project (201904d07020016), the Ministry of Science and Technology of China (Grant No. 2018YFC1603606), the project of the Intelligent Manufacturing Institute of HFUT (IMICZ2019007), the NSFC (No. 32172295, 21804028), the China Agriculture Research System-48 (CARS-48), the Anhui Provincial Natural Science Foundation (No. 1908085QC121), the China Postdoctoral Science Foundation (No. 225351), Suzhou S&T Committee Program (SNG2020056) and the Fundamental Research Fund for Central University (No. JZ2019HGTB0068).

Appendix A. Supplementary data

Supplementary data to this article can be found online at https://doi.org/10.1016/j.bios.2021.113804.

References

Anderson, G., Scott, M., 1991. Clin. Chem. 37, 398–402.
Chen, W., Cai, F., Wu, Q., Wu, Y.H., Yao, B.B., Xu, J.G., 2020. Food Chem. 328, 127081–127089.
Chen, W., Li, X.N., Wu, Q., Yao, L., Xu, J.G., 2019. Food Science & Human Wellness 8, 40–45.
Dalbeth, N., Merriman, T., 2009. Rheumatology 48, 222–226.
Dalbeth, N., Choi, H.K., Joosten, L.A.B., Khanna, P.P., Matsuo, H., Perez-Ruiz, F., Stamp, L.K., 2019. Nat. Rev. Dis. Primers 5, 69.
Erden, P.E., Kilic, E., 2013. Talanta 107, 312–323.
Fang, A., Wu, Q., Lu, Q., Chen, H., Li, H., Liu, M., Zhang, Y., Yao, S., 2016. Biosens. Bioelectron. 86, 664–670.
Fang, B., Feng, Y., Wang, G., Zhang, C., Gu, A., Liu, M., 2011. Microchim. Acta. 173, 27–32.
Fukuda, T., Muguruma, H., Iwasa, H., Tanaka, T., Hiratsuka, A., Shimizu, T., Tsuji, K., Kishimoto, T., 2020. Anal. Biochem. 590, 113533–113539.
Gao, X., Gui, R., Xu, K.Q., Guo, H., Jin, H., Wang, Z., 2018. New J. Chem. 42, 14796–14804.
Ge, J., Lei, J., Zare, R.N., 2012. Nat. Nanotechnol. 7, 428–432.
Grieshaber, D., MacKenzie, R., Vörös, J., Reimhult, E., 2008. Sensors 8, 1400–1458.
Hao, Y., Li, H., Cao, Y., Chen, Y., Lei, M., Zhang, T., Xiao, Y., Chu, B., Qian, Z., 2019. J. Biomed. Nanotechnol. 15, 951–965.
Huang, J., Zhu, X.L., Wang, Y.M., Ge, J.H., Liu, J.W., Jiang, J.H., 2018. Analyst 143, 4422–4428.
Khue, V.Q., Huy, T.Q., Phan, V.N., Tuan-Le, A., Thanh Le, D.T., Tonezzer, M., Hong Hanh, N.T., 2020. Mater. Chem. Phys. 255, 123562–123568.
Li, Y., Ran, G., Yi, W.J., Luo, H.Q., Li, N.B., 2012. Microchim. Acta. 178, 115–121.
Lou, D., Fan, L., Cui, Y., Zhu, Y., Gu, N., Zhang, Y., 2018a. Anal. Chem. 90, 6502–6508.
Lou, F., Wang, A., Jin, J., Li, Q., Zhang, S., 2018b. Electrochim. Acta 278, 255–262.
Lu, H.F., Li, J.Y., Zhang, M.M., Wu, D., Zhang, Q.L., 2017. Sensor. Actuator. B Chem. 244, 77–83.
Miland, E., Miranda Ordieres, A.J., Tuñón Blanco, P., Smyth, M.R., Fágáin, C.Ó., 1996. Talanta 43, 785–796.
Miller, P., Oberholzer, V., 1990. Clin. Chem. 36, 668–669.
Nishida, Y., 1992. Ann. Rheum. Dis. 51, 101–102.
Paraskos, J., Berke, Z., Cook, J., Miner, J., Braddock, M., Platt, A., Hughes, G., 2015. Expert Rev. Mol. Diagn. 66, 373–382.
Perelló, J., Sanchis, P., Grases, F., 2005. J. Chromatogr. B. 824, 175–180.
Ponnaiah, S.K., Periakaruppan, P., Vellaichamy, B., 2018. J. Phys. Chem. B 122, 3037–3046.
Revin, S.B., John, S.A., 2011. Electrochim. Acta 56, 8934–8940.
Saqib, M., Qi, L., Hui, P., Nsabimana, A., Halawa, M.I., Zhang, W., Xu, G., 2018. Biosens. Bioelectron. 99, 519–524.
Sheng, Y., Yang, H., Wang, Y., Han, L., Zhao, Y., Fan, A., 2017. Talanta 166, 268–274.
Shi, W., Li, J., Wu, J., Wei, Q., Chen, C., Bao, N., Yu, C., Gu, H., 2020. Anal. Bioanal. Chem. 412, 7275–7283.
Sun, L., Li, H., Li, M., Li, C., Li, P., Yang, B., 2016. J. Electroanal. Chem. 783, 167–175.
Vakh, C., Koronkiewicz, S., Kalinowski, S., Moskvin, L., Bulatov, A., 2017. Talanta 167, 725–732.
Verma, S., Choudhary, J., Singh, K.P., Chandra, P., Singh, S.P., 2019. Int. J. Biol. Macromol. 130, 333–341.
Wang, Q., Wen, X., Kong, J., 2020. Crit. Rev. Anal. Chem. 50, 359–375.
Wang, X., Yao, Q., Tang, X., Zhong, H., Qiu, P., Wang, X., 2019. Anal. Bioanal. Chem. 411, 943–952.
Wang, Y.R., Hu, P., Liang, Q.L., Luo, G.A., Wang, Y.M., 2007. Letture 18, 1111–1114.
Wang, Z., Guo, H., Gui, R., Jin, H., Xia, J., Zhang, F., 2018. Sensor. Actuator. B Chem. 255, 2069–2077.
Xin, X., Zhang, M., Zhao, J., Han, C., Liu, X., Xiao, Z., Zhang, L., Xu, B., Guo, W., Wang, R., Sun, D., 2017. J. Mater. Chem. C. 5, 601–606.
Xu, D.K., Hua, L., Li, Z.M., Chen, H.Y., 1997. J. Chromatogr. Biomed. Appl. 694, 461–466.
Yang, C., Zhang, Z., 2010. Talanta 81 (1), 477–481.
Ye, R., Zhu, C., Song, Y., Song, J., Fu, S., Lu, Q., Yang, X., Zhu, M.J., Du, D., Li, H., Lin, Y., 2016. Nanoscale 8, 18980–18986.
Zeinhom, M.M.A., Wang, Y., Sheng, L., Du, D., Li, L., Zhu, M.J., Lin, Y., 2018. Sensor. Actuator. B Chem. 261, 75–82.
Zen, J.M., Hsu, C.T., 1998. Talanta 46, 1363–1369.
Zhao, F.Y., Wang, Z.H., Wang, H., Zhao, R., Ding, M.Y., 2011. Chin. Chem. Lett. 22, 342–345.
Zhao, F., He, J., Li, X., Bai, Y., Ying, Y., Ping, J., 2020. Biosens. Bioelectron. 170, 112636–112643.